PALEOCEANOGRAPHY, VOL. 15, NO. 6, PAGES 731-737 DECEMBER 2000

Suppression of El Niño during the mid-Holocene by changes in the Earth's orbit

Amy C. Clement, Richard Seager, and Mark A. Cane
Lamont-Doherty Earth Observatory, Palisades, New York

Abstract. A number of recent reports have interpreted paleoproxy data to describe the state of the tropical Pacific, especially changes in the behavior of the El Niño-Southern Oscillation (ENSO), over the Holocene. These interpretations are often contradictory, especially for the eastern tropical Pacific and adjacent areas of South America. Here we suggest a picture of the mid-Holocene tropical Pacific region which reconciles the data. ENSO variability was present throughout the Holocene but underwent a steady increase from the mid-Holocene to the present. In the mid-Holocene, extreme warm El Niño events were smaller in amplitude and occurred less frequently about a mean climate state with a cold eastern equatorial Pacific and largely arid coastal regions as in the present climate. This picture emerges from an experiment in which a simple numerical model of the coupled ocean-atmosphere system in the tropical Pacific was driven by orbital forcing. We suggest that the observed behavior of the tropical Pacific climate over the mid- to late Holocene is largely the response to orbitally driven changes in the seasonal cycle of solar radiation in the tropics, which dominates extratropical influences.

1. Introduction

The possibility of changes in the behavior of the El Niño-Southern Oscillation (ENSO) with increased greenhouse gases in the atmosphere has been receiving increased attention. Clearly, changes in climate variability would have a substantial impact on human societies and ecosystems. Unfortunately, models disagree widely on what form those changes might take [*Meehl and Washington*, 1996; *Trenberth and Hoar*, 1996; *Rajagopalan et al.*, 1997; *Knutson et al.*, 1997; *Cane et al.*, 1997; *Timmerman et al.*, 1999; *Collins*, 2000]. One avenue for checking these future scenarios is to understand past ENSO variability.

Several recent studies have looked at changes in tropical Pacific climate during the Holocene period. *Rodbell et al.* [1999] presented a 15,000 year continuous record of deposition events from an alpine lake in Ecuador. Those authors report that interannual variability in the region was considerably weaker than in the modern climate prior to 7000 calendar years before present. This is consistent with various other proxies from the tropical Pacific region, which show a general increase in interannual variability into the late Holocene [*McGlone et al.*, 1992; *Shulmeister and Lees*, 1995].

Rodbell et al. [1999] argued that weaker ENSO variability during the mid-Holocene was due to a change in the mean state of the tropical Pacific. Fossil coral records from the Great Barrier Reef [*Gagan et al.*, 1998] and tropical ice cores from South America [*Thompson et al.*, 1995; 1998] indicate that in the mid-Holocene, parts of tropics were warmer than at present. Geoarchaeological data from sites in coastal Peru show the presence of certain tropical mollusk species between 8 and 5 kyr B.P. [*Sandweiss et al.*, 1996], which has been interpreted to indicate that the eastern equatorial Pacific was permanently warm at that time. Together with this data, *Rodbell et al.* [1999] cite results from a simplified model [*Sun*, 1999] to suggest that weaker ENSO variability in the mid-Holocene was due to a warmer tropical climate with a reduced equatorial gradient, implying an eastern equatorial Pacific that was significantly warmer than present at that time.

This view is called into question by data showing that coastal Peru and Chile were arid throughout the last 40 kyr [*Wells and Noller*, 1997]. If the eastern equatorial Pacific were permanently warm, one would expect the coastal regions of South America south of the equator to have strong seasonal rains every year, as in the coastal regions of Colombia to the north at the present time [*Peixoto and Oort*, 1993]. The Ecuadorian lake record would show increased sedimentation with significant clastic deposits. Instead, the bulk sedimentation rates are minimum in the mid-Holocene and increase toward the present. Results from coupled general circulation models do not agree with the *Rodbell et al.* [1999] view. A coupled general circulation model (CGCM) simulation of the climate at 6 kyr shows an enhanced equatorial gradient with a significantly cooler eastern equatorial Pacific [*Bush*, 1999]. Furthermore, the most recent CGCM studies of ENSO behavior under increasing CO_2 [*Timmerman et al.*, 1999; *Collins*, 2000] do

Paper number 1999PA000466.
0883-8305/00/1999PA000466$12.00

not support the contention that a warmer tropical Pacific climate would be steady or have a weak ENSO. While the causes for tropical Pacific warming would certainly be different for doubled CO_2 than for the mid-Holocene when atmospheric CO_2 concentrations were lower [*Crowley and North*, 1991], these CGCM experiments suggest that the relation between ENSO and mean state changes based on simple models [e.g. *Sun*, 1999] may not hold in the presence of more complete physics.

Here we offer a different picture of the tropical Pacific over the mid- to late Holocene. We suggest that the changes in ENSO are a response to orbitally driven changes in the seasonal cycle of solar radiation received at the surface of the tropical Pacific ocean. Modern ENSO events show a marked tendency to peak toward the end of the calendar year [*Rasmusson and Carpenter*, 1982], when the sea surface temperatures (SST) in the eastern equatorial Pacific are seasonally warming. Numerous studies with a hierarchy of models have shown that it is interactions between the seasonal cycle and interannual variability that give rise to ENSO [*Münnich et al*, 1991; *Chang et al.*, 1994; *Jin et al.*, 1994; *Tziperman et al.*, 1994; 1997]. Since the precession of the equinoxes alters the seasonal cycle of solar radiation in the tropics (Figure 1a), this is expected to influence ENSO behavior. Figure 1

2. Modeling Experiments

We imposed the orbitally induced changes in solar forcing as an anomalous heat flux (see Figure 1a) on the Zebiak-Cane coupled ocean-atmosphere model [*Zebiak and Cane*, 1987]. The top of the atmosphere values, derived as by *Berger* [1978], are reduced by a zonally uniform factor of 0.7 to account for the bulk effect of absorption and reflection of solar radiation by all atmosphere constituents. The changes in equatorial radiation over the Holocene are about half the magnitude as those of 65°N for July.

The Zebiak-Cane model has been used for more than a decade to understand and predict ENSO [*Cane*, 1986]. It is an anomaly model, with some aspects of the oceanic and atmospheric physics linearized about the monthly climatology of the present. The main dynamics in the atmosphere and ocean are described by linear shallow water equations on an equatorial beta plane. In the ocean an additional shallow frictional layer of constant depth (50 m) is included to account for the intensification of wind-driven currents near the surface. The time step of the ocean model is 10 days. At each time step the ocean and atmosphere are coupled through a parameterization of the atmospheric heating. The atmospheric heating anomaly is computed from the SST anomaly, the specified background surface wind divergence field, and the modeled divergence anomaly.

The model's active domain includes only the tropical Pacific (124°E to 80°W and 29°N to 29°S). Obviously, the omission of higher-latitude processes impairs its ability to fully simulate paleoclimatic variations. The simplicity of the model, however, simplifies interpretation: Its behavior is immediately attributable to ocean-atmosphere interactions in the tropical Pacific alone. Here we focus on the last 12,000 years of a 150,000 year experiment [*Clement et al.*, 1999] which can be compared with the continuous record provided by *Rodbell et al.* [1999].

An additional experiment is performed in which the top of the atmosphere solar radiation is converted into a surface forcing in a way that accounts for observed cloud cover, which is greater in the western Pacific than in the east. This spatially dependent factor is calculated as the ratio of the annual mean surface solar insolation to the top of the atmosphere values in the National Centers for Environmental Prediction (NCEP) reanalysis product [*Kalnay et al.*, 1996]. The results of this experiment are qualitatively the same as those with the spatially uniform solar forcing and will not be discussed.

3. Results

Rodbell et al. [1999] show that moderate to severe El Niño events of the past century roughly coincide with the appearance of clastic laminae in the lake record. The clastic laminae are more frequent after 7 ka, though the increase appears to be continuous over the 15 kyr. To compare the model results with this record, we compute the frequency and amplitude of warm ENSO events within 500 year overlapping windows (Figure 2). Figure 2 A large event is defined to occur when the mean December-February NINO3 index (the average SST anomaly over the region 150°W to 90°W and 5°S to 5°N) exceeds 3°C. This index corresponds to the middle of the rainy season in coastal South America during which SST anomalies associated with ENSO are largest and are responsible for the equatorward migration of the Intertropical Convergence Zone (ITCZ) and large precipitation anomalies in the region. The model results show a distinct increase in both the frequency and amplitude of warm ENSO events over the mid- to late Holocene. The trends in event frequency and amplitude are computed for the period from 10 kyr to the present and compared with the trends over 10 kyr periods from a 60 kyr year run with orbital parameters fixed at modern values. The trend in the orbitally forced run in event frequency per 500 years, calculated using a linear least squares fit, is 41/10,000 years and in mean event amplitude is 0.35/10,000 years (see Figure 2). The control run is split into 50 overlapping 10,000 year windows for which a mean trend and standard deviation are computed. The orbitally driven trend in event frequency (amplitude) is 5.6 (17.5) standard deviations away from

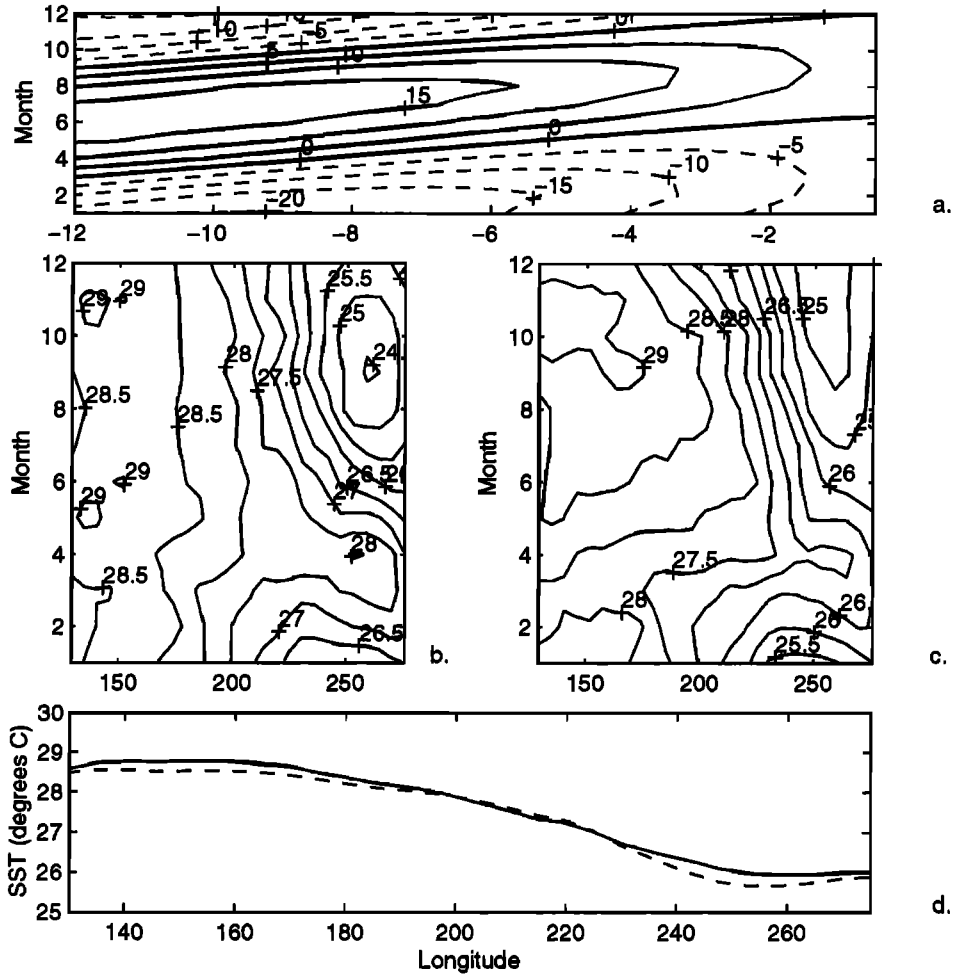

Figure 1. (a) Contour plot of the anomalous surface solar radiation on the equator (W m^{-2}) that is used to force the Zebiak-Cane coupled ocean-atmosphere model. The surface solar radiation is computed from the top of atmosphere values [*Berger*, 1978] assuming a fixed atmospheric transmissivity with a value of 0.7 meant to represent the bulk effect of absorption and reflection of solar radiation by all atmosphere constituents, and the solar zenith angle is also calculated as by *Clement et al.* [1999]. Values are plotted as a function of kiloyears before present (X axis) and month of the year (Y axis). The contour interval is 5 W m^{-2}. (b) Seasonal cycle of SST on the equator for the present climate as a function of month (Y axis). Note that this consists of both the background mean SST as well as the mean anomaly SST which is non zero due to the skewness of warm events (*Zebiak and Cane*, 1987). (c) Same as Figure 1b but with the anomalous seasonal cycle for the mid-Holocene (8-6 kyr) added to the present-day background seasonal cycle. (d) Annual mean SST along the equator for the present day (solid) and the mid-Holocene (dashed).

the mean of the unforced case, making these trends statistically different at greater than the 99% confidence level. Thus the orbital forcing changes ENSO in such a way that both the change in the frequency and magnitude of warm events over the Holocene are distinct from the unforced variability of the system. Both of these changes in the character of warm events would reduce the occurrence of large precipitation anomalies over coastal Ecuador in the mid-Holocene relative to the modern and are therefore consistent with the sedimentation record of the Ecuadorian lake.

Since the model is forced only by orbital changes, with no change in mean state, the explanation for the change in the behavior of the model ENSO lies in the change in the seasonal cycle. Presently, the Earth passes through the point of its orbit closest to the Sun (perihelion) at the beginning of the calendar year. During the mid-Holocene, when the ENSO variability was weaker, perihelion occurred in the middle of the calendar year (Figure 1a). Consequently, the equatorial oceans received less heat during boreal winter (Figures 1b and 1c), which contributes to the smaller event amplitudes during that season (Figure 2b).

The change in ENSO behavior involves the response of the coupled dynamics to the solar forcing. By itself the thermodynamic response to the orbital forcing at

the surface of the ocean produces a zonally uniform seasonal SST anomaly. The response of the atmosphere to SST anomalies is larger in the western part of the basin, where the year-round presence of warm SST and atmospheric convection converts the SST anomaly into a deep atmospheric heating anomaly, than in the east, where cooler SST and mean descending motion suppress convection throughout much of the year. The zonally symmetric heating associated with the solar forcing therefore generates a larger atmospheric heating response in the west than in the east, which drives an easterly wind anomaly.

While the asymmetry in the atmospheric response to a zonally uniform forcing prevails throughout the year, the resulting wind anomalies have a different effect on ENSO behavior depending on the season. Warm ENSO events tend to develop rapidly in the summer and fall [*Rasmusson and Carpenter*, 1982] when the system is most unstable to ENSO-like perturbations [*Zebiak and Cane*, 1987; *Blumenthal*, 1991; *Xue et al.*, 1997]. In the mid-Holocene the heating of the coupled system in the boreal summer introduces an easterly wind anomaly. This wind field anomaly sets off a chain of positive feedbacks between the atmosphere and ocean which, within several months, tend to cool the eastern equatorial Pacific via the same coupled interactions that give rise to ENSO [*Bjerknes*, 1969]. This is demonstrated in Figure 3, which shows the evolution of a typical warm event in the model with modern solar forcing compared with a run using the same initial conditions but with the June-August mid-Holocene forcing (and zero forcing the rest of the year). Figure 3 These experiments isolate the effect of the boreal summer forcing on ENSO. In both runs a warm event develops in the late spring. The heating during boreal summer initially produces an additional warming relative to the unforced case (Figure 3a). However, this warming introduces an easterly wind anomaly in the central Pacific (Figure 3b) owing to the zonally asymmetric response to the heating of the atmosphere. This wind anomaly generates a cooling tendency in the eastern equatorial Pacific by September. Because this is the season when events tend to develop rapidly, the growth of El Niño events is inhibited. The result is that fewer large warm events occur in the presence of this boreal summer forcing.

We note that in this model, the cold ENSO events (La Niñas) are not as tightly phase locked to the seasonal cycle as the warm events. Furthermore, strong cold events tend to follow strong warm events [*Zebiak and Cane*, 1987]. Thus the response of the model ENSO to the seasonal forcing is dominated by the effect on the warm events. Since the occurrence of large warm events is reduced in the mid-Holocene, the occurrence of cold events is also reduced. As the solar forcing approaches modern values, the numbers of warm events and cold events both increase.

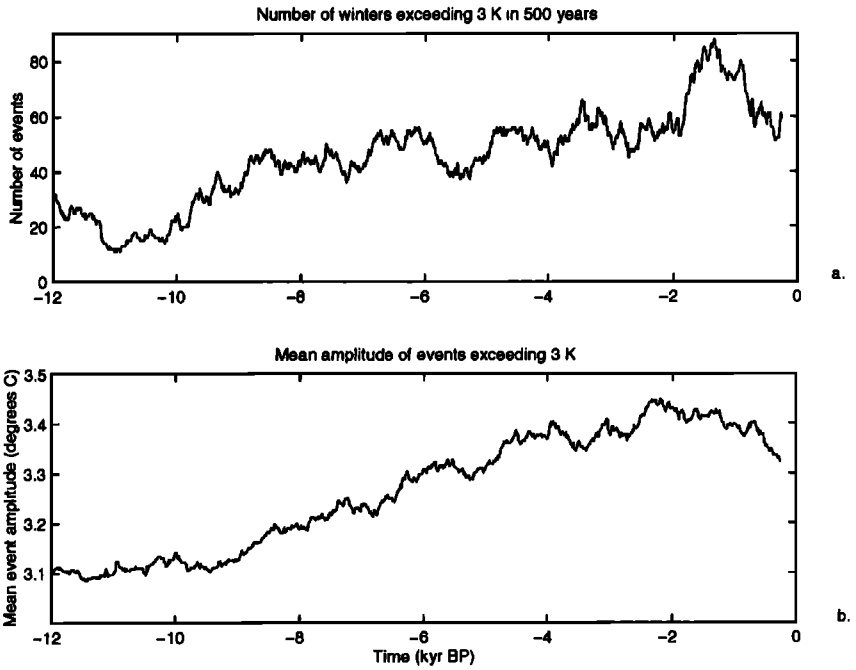

Figure 2. (a) The number of occurrences of events in 500 year overlapping windows (overlapping every 10 years) as a function of kiloyears B.P. An eve nt is defined to occur when the mean December-February NINO3 SST anomaly exceeds 3 K. (b) The mean amplitude in the same overlapping 500 year windows of the events exceeding 3 K (in °C).

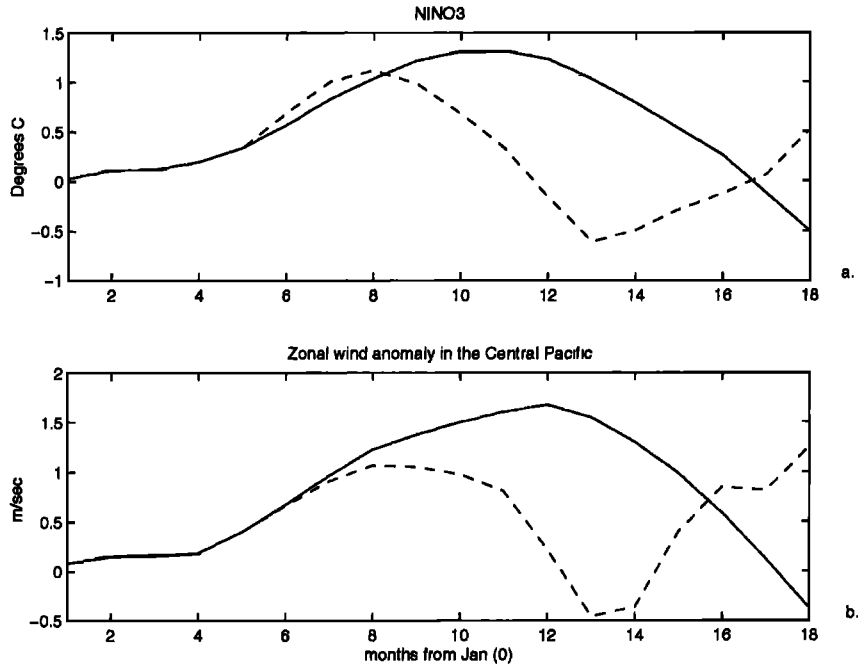

Figure 3. The evolution of a typical event for the modern solar forcing (solid line) and the mid-Holocene solar forcing in June-August and zero forcing during the rest of the year (dashed line). The two experiments have identical initial conditions and the first year and a half (starting in January (0)) are shown in (a) the NINO3 index and (b) the zonal wind field anomaly on the equator in the central Pacific (180°E to 140°W) in m s^{-1}.

4. Discussion

The model results presented here demonstrate how orbitally driven changes in the seasonal cycle alter ENSO behavior over the Holocene in a way that is consistent with the Ecuadorian lake record [*Rodbell et al.*, 1999] and the evidence that the coastal regions of Peru and Chile have been arid for the last 40kyr [*Wells and Noller*, 1997]. We suggest that the orbital configuration in the mid-Holocene, a time of greater heating in the boreal summer and less heating in boreal winter, altered the seasonal cycle of the coupled system such that the development of warm events was suppressed. The system continued to oscillate throughout the Holocene, though large warm events occurred less frequently and were smaller in magnitude in the mid-Holocene. This implies fewer large fluvial events in Ecuador, accounting for the decreased clastic laminae at that time observed by *Rodbell et al.* [1999]. In the mid-Holocene, parts of the tropics may have been warmer, as suggested by *Gagan et al.* [1998] and *Thompson et al.* [1995; 1998], but the eastern equatorial Pacific was cold, as in the present climate (Figure 1d), which is consistent with persistent dry conditions on the coast, as by *Wells and Noller* [1997].

The presence of certain mollusk fauna that are typical of warm waters between 8 and 6 ka in coastal regions of Peru and Chile observed by *Sandweiss et al.* [1996] remains to be explained. The purely thermodynamic response of the tropical ocean to the mid-Holocene solar forcing damps the present-day seasonal cycle in the eastern equatorial Pacific. Cooling induced by the solar forcing occurs in the boreal winter and spring when SST are seasonally warm in the modern ocean, while heating occurs when SST are seasonally cool in the boreal summer and early fall. This has the effect of increasing the cold season SST by about half a degree (Figures 1b and 1c). Furthermore, in the model run, there are fewer extreme cold events associated with the change in ENSO behavior in the mid-Holocene, which is consistent with an increase in climate variability into the late Holocene that has been noted in other proxies from the tropical Pacific [*McGlone et al.*, 1992; *Shulmeister and Lees*, 1995]. These results indicate that cold climate conditions, both seasonally and interannually, were less likely to occur in the mid-Holocene. Perhaps this reduction in extreme cold temperatures accounts for the survival of tropical mollusks as found by *Sandweiss et al.* [1996]. It has been argued that these thermally anomalous molluscan assemblages are due to changes in coastal geomorphology and sea level rise rather than large scale climate change [*DeVries et al.*, 1997]. This raises the possibility that coastal temperatures may change independently from the large scale tropical Pacific climate. *Montoya et al.* [2000] have argued, on the basis of experiments with a CGCM for the period 125 ka, that a

"mini-monsoonal" circulation over South America can be induced by changes in the orbital forcing resulting in coastal warming. *Liu et al.* [1999] have also found that warming in the mid-Holocene could be confined to the coastal region, while the central/eastern equatorial Pacific cools. Models that better represent the physics of coastal processes and which include a seasonal cycle are needed to address the issue of changes in mollusk populations properly.

The model used in this study is highly idealized, omitting many of the processes that could influence ENSO behavior. Some of these include the mean SST and zonal gradients within the equatorial Pacific [*Battisti and Hirst*, 1989; *Sun and Liu*, 1996; *Sun*, 1999], conditions in the North Pacific Ocean [*Mantua et al.*, 1997; *Kleeman et al.*, 1999], and the Asian monsoon [*Shukla and Paolina* 1983]. Recent studies with more complete models (CGCM) have been performed to investigate the change in the tropical Pacific under 6 ka orbital configuration. These experiments [*Bush et al.*, 1999; *Otto-Bliesner*, 1999, *Liu et al.*, 1999] are too short to resolve these subtle changes in ENSO behavior [see *Cane et al.*, 1995]. *Liu et al.* [2000] have done further experiments at 11 ka and find some indication that orbitally driven changes in the Asian monsoon may reduce ENSO variability in the early to mid-Holocene. The issue of how ENSO behaves in CGCMs in response to changes in orbital forcing awaits longer experiments.

There are possibly other things at play besides the solar forcing in the changes of the ENSO system over the Holocene. Many aspects of the climate were changing over this period, including global sea level, temperature, monsoon strength, and high-latitude ice cover [*Crowley and North*, 1991]. However, the model results presented here show that the altered seasonal cycle due to the orbital forcing alone is capable of leading to a steady increase in ENSO variability from the mid-Holocene to the present. This idea must be further explored with records of past climate variability from the tropical Pacific. Fossil corals, in particular, are potential means for unraveling the changes in the behavior of ENSO over the Holocene.

Acknowledgments. The authors thank H. Loukos, A. Juillet-Leclerc, and P. deMenocal for their comments. The comments of D. Battisti, T. Crowley, and Z. Liu were also very helpful. A.C. gratefully acknowledges Pascale Delecluse for her support. R.S. is supported by NASA grant NAGW -916 and NOAA grant UCSIO -10775411D/NA47GP0188 (The Consortium on the Oceans Role in Climate). M.A.C. is supported by NOAA grant NA36GP0074-02. This is a Lamont Contribution number 6087.

References

Battisti, D. S., and A. Hirst, Interannual variability in the tropical atmosphere/ocean system: Influence of the basic state and ocean geometry, *J. Atmos. Sci.*, *46*, 1687–1712, 1989.

Berger, A., Long-term variations of daily insolation and Quaternary climate changes, *J. Atmos. Sci.*, *35*, 2362–2367, 1978.

Bjerknes, J., Atmospheric teleconnections from the equatorial Pacific, *Mon. Weather. Rev.*, *97*, 163–172, 1969.

Blumenthal, M. B., Predictability of a coupled ocean-atmosphere model, *J. Clim.*, *4*, 766–784, 1991.

Bush, A.B.G., Assessing the impact of mid-Holocene insolation on the ocean-atmosphere system, *Geophys. Res. Lett.*, *26*, 99–102, 1999.

Cane, M., El Niño, *Annu. Rev. Earth Planet Sci.*, *14*, 43–70, 1986.

Cane, M. A., S. Zebiak, and Y. Xue, Model studies of long-term behavior of ENSO, in *Natural Climate Variability on Decadal-to-Century Time Scales*, pp. 442–457, Nat. Res. Council, Washington, D. C., 1995.

Cane, M. A., A. C. Clement, A. Kaplan, Y. Kushnir, D. Pozdnyakov, R. Seager, S. E. Zebiak, and R. Murtugudde, Twentieth century sea surface tempature trends, *Science*, *275*, 957–960, 1997.

Chang, P., B. Wang, T. Li, and L. Ji, Interactions between the seasonal cycle and the Southern Oscillation: Frequency entrainment and chaos in a coupled ocean-atmosphere model, *Geophys. Res. Lett.*, *21*, 2817–2820, 1994.

Clement, A. C., R. Seager, and M. A. Cane, Orbital controls on the tropical climate, *Paleoceanography*, *14*, 441–456, 1999.

Collins, M., The El Niño Southern Oscillation in the second Hadley Centre coupled model and its response to greenhouse warming, *J. Clim.*, *13*, 1299–1312, 2000.

Crowley, T., and G. North, *Paleoclimatology*, Oxford Univ. Press, New York, 1991.

DeVries, T. J., L. Ortlieb, and A. Diaz, Determining the early history of ENSO, *Science*, *276*, 965–966, 1997.

Gagan, M., L. Ayliffe, D. Hopley, J. Cale, G. Mortimer, J. Chappell, M. McCulloch, and M. Head, Temperature and surface-ocean water balance of the mid-Holocene tropical western Pacific, *Science*, *279*, 1014–1018, 1998.

Jin, F.-F., J. D. Neelin, and M. Ghil, El Niño on the Devil's staircase: Annual subharmonic steps to chaos, *Science*, *264*, 70–72, 1994.

Kalnay, E., et al., The NCEP/NCAR 40 year reanalysis project, *Bull. Am. Meteorol. Soc.*, *77*, 437–471, 1996.

Kleeman, R., J. McCreary, and B. Klinger, A mechanism for generating ENSO decadal variability, *Geophys. Res. Lett.*, *26*, 1743, 1999.

Knutson, T. R., S. Manabe, and D. Gu, Simulated ENSO in a global coupled ocean-atmosphere model: Multidecadal amplitude modulation and CO_2 sensitivity, *J. Clim.*, *10*, 131, 1997.

Liu, Z., R. Jacob, J. Kutzbach, S. Harrison, and J. Anderson, Monsoon impact on El Niño in the early Holocene, *PAGES Newsl*, *7*, 16–17, 1999.

Liu, Z., J. Kutzbach and L. Wu, Modeling the climatic shift of El Nino variability in the Holocene, *Geophys. Res. Lett.*, in press, 2000.

Mantua, N., S. Hare, Y. Zhang, J. Wallace, and R. Francis, A Pacific interdecadal climate oscillation with impacts on Salmon production, *Bull. Am. Meteorol. Soc.*, *78*, 1069–1079, 1997.

McGlone, M., A. P. Kershaw, and V. Margraf, El Niño/Southern Oscillation climatic variability in Australasian and South American paleoenvironmental records, in *El Niño. Historical and Paleoclimatic Aspects of the Southern Oscillation*, edited by H. Diaz and V. Margraf, pp. 435–462, Cambridge Univ. Press, New York, 1992.

Meehl, G., and W. Washington, El Niño-like climate change in a model with

increased atmospheric CO_2 concentrations., *Nature*, *382*, 56–60, 1996.

Montoya, M., H. von Storch, and T. J. Crowley, Climate simulation for 125,000 years ago with a coupled ocean-atmosphere general circulation model, *J. Clim.*, *13*, 1057–1072, 2000.

Münnich, M., M. A. Cane, and S. E. Zebiak, A study of self-excited oscillations of the tropical ocean atmosphere system, II, Nonlinear cases, *J. Atmos. Sci.*, *48*, 1238–1248, 1991.

Otto-Bliesner, B., El Niño/La Niña and Sahel precipitation during the middle Holocene, *Geophys. Res. Lett.*, *26*, 87–90, 1999.

Peixoto, J. P., and A. H. Oort, *Physics of Climate*, Am. Inst. of Phys., New York, 1993.

Rajagopalan, B., U. Lall, and M.A. Cane, Anomalous ENSO occurences: An alternate view, *J. Clim.*, *10*, 2351–2357, 1997.

Rasmusson, E., and T. Carpenter, Variations in tropical sea surface temperature and surface wind fields associated with the Southern Oscillation/El Niño, *Mon. Weather Rev.*, *110*, 354–384, 1982.

Rodbell, D., G. Seltzer, D. Anderson, M. Abbott, D. Enfield, and J. Newman, An 15,000 year record of El Niño-driven alluviation in southwestern Ecuador, *Science*, *283*, 516–520, 1999.

Sandweiss, D., J. Richardson, E. Reitz, H. Rollins, and K. Maasch, Geoarchaeological evidence from Peru for a 5000 year B.P. onset of El Niño, *Science*, *273*, 1531–1533, 1996.

Shukla, J., and D. Paolina, The Southern Oscillation and long range forecasting of the summer monsoon rainfall over India, *Mon. Weather Rev.*, *111*, 1830–1837, 1983.

Shulmeister, J., and B. Lees, Pollen evidence from tropical Australia for the onset of an ENSO dominated climate at c. 4000 BP, *Holocene*, *5*, 10–18, 1995.

Sun, D.-Z., Global climate change and El Niño: A theoretical framework, in *El Niño and the Southern Oscillation: Multiscale Variability, Global and Regional Impacts*, edited by H. F. Diaz and V. Margraf, p. 443-463, Cambridge Univ. Press, New York, 1999.

Sun, D.-Z., and Z. Liu, Dynamic ocean-atmosphere coupling: A thermostat for the tropics, *Science*, *272*, 1148–1150, 1996.

Thompson, L., E. Mosley-Thompson, M. E. Davis, P.-N. Lin, K. A. Henderson, J. Cole-Dai, J. F. Bolzan, and K. b. Liu, Late glacial stage and Holocene tropical ice core records from Huascaran, Peru, *Science*, *269*, 46–50, 1995.

Thompson, L., et al., A 25,000-year tropical climate history from Bolivian ice cores, *Science*, *282*, 1858–1864, 1998.

Timmermann, A., J. Oberhuber, A. Bacher, M. Esch, M. Latif, and E. Roeckner, ENSO response to greenhouse warming, *Nature*, *398*, 694, 1999.

Trenberth, K., and T. J. Hoar, The 1990-1995 El Niño-Southern Oscillation event: Longest on record, *Geophys. Res. Lett.*, *23*, 57-60, 1996.

Tziperman, E., M. A. Cane, and S. E. Zebiak, Irregularity and locking to the seasonal cycle in an ENSO prediction model as explained by the quasi-periodicity route to chaos, *J. Atmos. Sci.*, *52*, 293–306, 1994.

Tziperman, E., S. E. Zebiak, and M. Cane, Mechanisms of seasonal-ENSO interaction, *J. Atmos. Sci.*, *54*, 61–71, 1997.

Wells, L. E., and J. S. Noller, Determining the early history of ENSO, *Science*, *276*, 966–966, 1997.

Xue, Y., M.A. Cane, and S.E. Zebiak, Predictability of a coupled model of ENSO using singular vector analysis, Part I, Optimal growth in seasonal background and ENSO cycles, *Mon. Weather Rev.*, *125*, 2043–2056, 1997.

Zebiak, S. E., and M. A. Cane, A model El Niño-Southern Oscillation, *Mon. Weather Rev.*, *115*, 2262–2278, 1987.

M.A. Cane, A.C. Clement and R. Seager, Lamont-Doherty Earth Observatory, Route 9W, Palisades, New York 10964. (e-mail: clement@rosie.ldeo.columbia.edu)

(Received October 13, 1999;
revised April 3, 2000;
accepted May 18, 2000.)